Neural Activity from Attention Networks Predicts Movement Errors

Macauley Smith Breault[1], Jorge A. González-Martínez[2], John T. Gale[3], and Sridevi V. Sarma,[1]*IEEE Member*

***Abstract*— Traditionally, movement-related behavior is estimated using activity from motor regions in the brain. This predictive capability of interpreting neural signals into tangible outputs has led to the emergence of Brain-Computer Interface (BCI) systems. However, nonmotor regions can play a significant role in shaping how movements are executed. Our goal was to explore the contribution of nonmotor brain regions to movement using a unique experimental paradigm in which local field potential recordings of several cortical and subcortical regions were obtained from eight epilepsy patients implanted with depth electrodes as they performed goal-directed reaching movements. The instruction of the task was to move a cursor with a robotic arm to the indicated target with a specific speed, where correct trials were ones in which the subject achieved the instructed speed. We constructed subject-specific models that predict the speed error of each trial from neural activity in nonmotor regions. Neural features were found by averaging spectral power of activity in multiple frequency bands produced during the planning or execution of movement. Features with high predictive power were selected using a forward selection greedy search. Using our modeling framework, we were able to identify networks of regions related to attention that significantly contributed to predicting trial errors. Our results suggest that nonmotor brain regions contain relevant information about upcoming movements and should be further studied.**

I. INTRODUCTION

Neuroscientists who study sensorimotor control have typically conducted experiments wherein they train animals or humans to make specific movements, and record corresponding brain activity in motor cortical regions in addition to behavior. Researchers have achieved great success in using neural activity from motor regions to estimate observed behavior using models [1]. More impressive is the fact that this information can be estimated using activity prior to or during movement [2].

This capability of reliably translating neural activity into observable actions is of great interest for applications such as Brain-Computer Interfaces (BCIs) [2]. Most BCIs tend to rely on neural activity recorded from the primary motor cortex and premotor cortex. Fluent motor control, however, relies on the communication between motor and nonmotor regions for the integration of sensory information and the attenuation of movement [3]. Further, nonmotor regions also have the predictive capability to decode epoch, direction, or performance [4], [5], which can be combined with activity from motor regions to improve BCI performance [2].

Gaining access to nonmotor regions is no easy task. Most of these regions are deep structures which are difficult to access, particularly in humans. Noninvasive approaches, such as fMRI, have been used to depict activity over the entire brain [6], [7]. However, these data lack fine temporal resolution in that images are taken every 1–2 s, while reactions to cues and movements themselves may happen on the order of milliseconds [8]. Invasive recordings, on the other hand, have a fine temporal resolution but are typically extracted from one or a small set of brain regions. The spectral content of Local Field Potential (LFP) activity recovered using depth electrodes have been shown to decode behavior as well as single unit activity and sustain more stable activity over time [9], [10].

Building an interesting model that relates brain to behavior starts with an interesting data set. Here, we recorded neural activity from superficial to deep nonmotor brain regions of eight human epilepsy subjects clinically implanted with depth electrodes for clinical purposes. Subjects played a game by making sequential goal-directed center-out reaching movements with an instructed speed. Neural data were recorded using stereoelectroencephalography (SEEG) technique to render the Local Field Potential (LFP) activity, which communicates information across the brain at a population-level [11].

Our study shows one can predict behavior using these regions with an average prediction error of 0.89 ± 0.09 (mean $\pm$ standard deviation). Specifically, we found that regions related to attention and performance monitoring were able to predict speed error across multiple subjects. Although preliminary, the results of our model suggest the involvement of nonmotor brain regions during the planning and execution of reaching movements and their impact on performance.

II. METHODS

A. Subjects

Eight individuals over the age of 18 with medically refractory epilepsy who could provide informed consent were recruited for this study. These subjects were undergoing surgery to find the epileptogenic zone for possible resection at Cleveland Clinic were recruited for this study with informed consent. Their enrollment was completely voluntary. These experimental protocols were approved by the Institutional Review Board and methods were carried out

*This work was supported by a National Science Foundation grant (EFRI-MC3: # 1137237) awarded to J. A. G., J. T. G., and S. V. S., NIH R01 NS110423 to S. V. S., and M. S. B. thanks the ARCS Foundation for their generous support.

[1]Macauley Smith Breault and Sridevi V. Sarma are with the Department of Biomedical Engineering, Johns Hopkins University, Baltimore, MD 21218, USA mbreaul1@jhu.edu

[2]Jorge A. González-Martínez is with the Department of Neurosurgery, Cleveland Clinic, Cleveland, OH 44195, USA

[3] John T. Gale is with Gale Neurotechnologies Inc., Smoke Rise, GA 30087, USA

in accordance with approved guidelines. This study did not alter their clinical care, other than performing the behavioral experiments.

B. SEEG Implantation

The implantation of the SEEG depth electrodes (PMT Corporation, MN, USA) was performed at the Cleveland Clinic. Each subject was implanted stereotactically with approximately 8–13 depth electrodes using a robotic surgical implantation platform (ROSA, Medtech Surgical Inc., USA) [12]. Specific implantation locations were planned prior to surgery with coregistered three-dimensional CT and MRI scans. Locations included lateral, intermediate, and/or deep cortical and subcortical structures [12]. Postoperative images were used to label the anatomical location of contacts along each electrode with the approval of at least two clinical experts.

C. Electrophysiological Recordings

The raw neural data were in the form of local field potential activity from superficial to deep nonmotor brain structured. Neural recordings were collected onsite using a clinical electrophysiology acquiring system (Nihon Kohden 1200, Nihon Kohden America, USA) in the Epilepsy Monitoring Unit at a sampling rate of 2 kHz. The recording sessions were checked to make sure they were free of epileptic activity.

D. Motor Task

Subjects performed speed- and goal-directed reaching movements previously described in [13], [14], [15]. Movements in a horizontal plane were made and monitored with a robotic manipulandum from the InMotion ARM Interactive Therapy System (Interactive Motion Technologies, Watertown, MA, USA). Visual feedback was displayed on an attached computer screen, where hand location appeared as a cursor. The task interface was prepared using MonkeyLogic in MATLAB® (Mathworks, Natick, MA) [16].

Subjects first performed calibration trials in order to get comfortable using the manipulandum and to also record their fasted speed to scale speeds during the experiment. Trials started by presenting the speed instruction before subjects reoriented their cursor to a circle in the center. Once at the center, a target would appear either to the left, right, above, or below the center. The time between target appearance and movement cue was marked as *planning*. Movements were cued when the target changed to green after a random delay 2.00 ± 0.25 s. The time between movement initiation but prior to target acquisition was marked as *execution*. During 20 % of the trials, a perturbation with a random magnitude and direction was applied using the robotic manipulandum. Subjects were expected to attain the instructed speed despite perturbations. After holding the cursor in the target for 0.5 s, their actual speed (scaled by their calibration speed) were shown relative to the instructed speed as feedback. Successful trials were followed by a picture of a $5 bill while unsuccessful trials were shown a picture of a $5 bill overlaid with a red X.

E. Data Preparation

1) Neural Data: The neural data were preprocessed using spectral analysis with custom MATLAB® scripts. Oscillatory power was calculated using continuous wavelet transform on a logarithmic scale vector between 1–200 Hz and complex Morlet wavelet with $\omega_0 = 6$. The instantaneous power spectral density was then averaged across overlapping time bins (50 %) with a time window of 100 ms every 50 ms. Each time bin was labeled as the last corresponding temporal index. Finally, the logarithm of the power in each frequency was normalized using the mean and standard deviation over the entire recording session. Contacts with abnormal bursting activity were ignored.

2) Movement Data: Actual speeds were compared to the instructed speed after each completed movement. Speeds were scaled between $[0, 1]$, where speeds equal to or above their calibration speed were capped at 1. For the trial to be successful, the scaled actual speed must fall within a range: 0.20–0.47 for slow trials or 0.53–0.80 for fast trials. The speed error was found by taking the difference between their actual and instructed speed per trial, such that trials that were too fast had a positive error. Errors were then normalized using the standard score in preparation for modeling.

Trials with incomplete movements were ignored. Only trials without perturbations were used for the purposes of this paper, as perturbed trials generally lead to incorrect speeds for reasons that are not completely in control of the subject. On average, subjects performed 96 ± 33 completed, unperturbed trials.

F. Encoding Model and Decoding Procedure

Our goal was to build a model that could predict the error of the speed a subject would make on a trial-by-trial basis only using neural activity. This is a typical regression problem, where the output variable is the *speed errors*, which are continuous values, and the features consist of spectral power in different frequency bands of the *neural activity* from a selected set of electrode contacts.

Trials were split into training and testing sets using a 90–10 split. The training set was used to construct a model for each subject, i.e., select features and fit coefficients, and the testing set was used to test the performance of the model on new data. We built two models for each subject: one using neural activity from planning as features and the other using neural activity from execution as features.

1) Encoding Error: Subject-specific models were built that used neural activity during planning or execution to predict their speed error on a trial-by-trial basis Assume error for subject n on trial t is a random variable denoted as $y_n(t) \in \mathbb{R}$. Then, error is a random variable with a Gaussian distribution, whose mean depends on a vector of features $\mathbf{x}_n(t) \in \mathbb{R}^{J_n}$:

$$\mathbb{E}[y_n(t) \mid \mathbf{x}_n(t)] = \beta_{n0} + \sum_{j=1}^{J_n} \beta_{nj}\, x_{nj}(t), \tag{1}$$

where $\beta_{n0} \in \mathbb{R}$ is the baseline error, $\beta_{nj} \in \mathbb{R}$ is the coefficient on the feature, and $x_{nj}(t)$ captures the average spectral power of neural activity from electrode contact j on trial t.

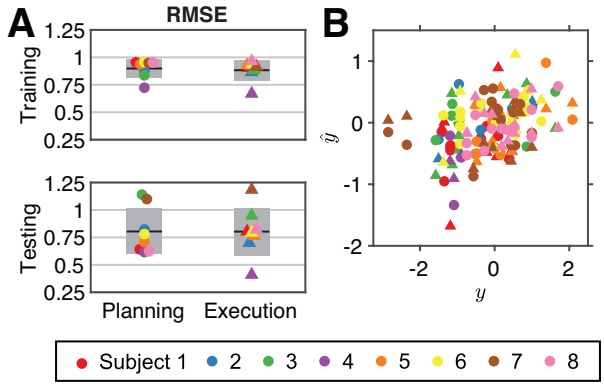

Fig. 1. **A** RMSE on training (top) and testing (bottom) set for planning and execution models. Each subject is distinguished by a different color, with the mean (black solid line) and one standard deviation (grey rectangle). **B** Scatter plot of observed (y) and predicted speed error ($\hat{y}$) using planning (circles) and execution model (triangles) on trials from the testing set.

2) Feature Selection and Model Fitting: Features for each model consisted of the average spectral content of neural activity across multiple frequency bands, including theta (4–8 Hz), alpha (8–15 Hz), beta (15–30 Hz), low gamma (30–60 Hz), high gamma (60–100 Hz), and hyper gamma (100–200 Hz) [17], [18], [19], [20], [21], [22]. Features for planning models were found using a time window around planning (1.75 s) while features for execution models were found using a time window around execution (0.52 ± 0.26 s). The full feature vector for each trial then consisted of the six average powers from each frequency band for each electrode contact. A forward selection data-driven approach was employed to select the most influential features for each model [23]. Features were added in a stepwise fashion using the `stepwiseglm` function in MATLAB®, which begins with an intercept and incrementally adds/removes features that improved the Akaike Information Criterion for a maximum of `nstep` $= 2$. Selecting features in this manner retained the interpretability of each model as it pertained too connecting features to the outputs.

Trials were partitioned into training and testing sets in such a way that both sets preserved the properties of the original distributions of speed errors. We decided to use 90 % of the trials for training and the remaining 10 % for testing. After partitioning the data, a planning and execution model were constructed for each subject n. Model construction consists of selecting features from the appropriate full feature vector and fitting coefficients using `glmfit` on the training set. This fitted model can then be used to predict the speed error, $\hat{y}_n(t)$, on trial t. Specifically, models were tested using trials from the testing set, which are independent of the trials used for training. The performance of each model on the training and testing set was measured using the Root-Mean-Squared Error (RMSE).

3) Feature Mapping: Model features were highlighted onto a human MRI atlas [24]. This was done by matching the associated label of each feature to the atlas. Regions that were recorded from but not selected as a feature were hatched. Features that could not be matched to the atlas were ignored for visualization.

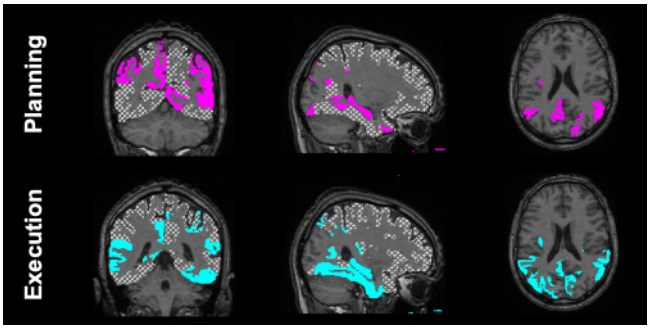

Fig. 2. Map of features that predict trial error using neural activity from planning (top) and execution (bottom). The label of the electrode contacts for each feature was matched to labels from the Mori atlas [24]. Regions, where a subject had contacts that were not featured in a model, were filled in using a hatched grey area. Note that these maps do not represent fMRI signals nor do they represent the exact location of electrodes.

III. RESULTS

A. Performance

Fig. 1A displays the performance of all the models on the training and testing sets. The average RMSE across all subjects decreases from the training to the testing set but is more variable. Specifically, the average error on the training set was 0.90 ± 0.08 and 0.88 ± 0.09 for the planning and execution model, respectively, compared to 0.80 ± 0.21 and 0.80 ± 0.22 on the testing set. This indicates that the models generalize well when tested on new data for most subjects.

Fig. 1B demonstrates how well the models predict speed error compared to what was actually observed. Namely, all models produce comparable positive linear relationship both between planning and execution and across subjects, indicating that they all capture a similar trend. Based on our quantitative and qualitative measurements, the planning and execution models comparably predict speed error well across subjects.

B. Features

All features identified across models were matched to their associated label and highlighted onto MRI slices in Fig. 2. We were interested in whether any regions were identified as a feature consistently within and between planning and execution as well as across subjects. This process generated a list of features for the discussion. Features from planning that were common across multiple subjects included the angular gyrus, cingulate cortex, and hippocampus. Execution features that were common across multiple subjects included the hippocampus and superior temporal gyrus. Finally, common features between the planning and execution models included angular gyrus, cingulate cortex, hippocampus, and insular cortex.

IV. DISCUSSION

In this study, we sought to identify whether, if any, nonmotor regions in our data could predict speed error on any given trial. These regions have been suggested to improve performance BCI during movement but the exact information they provided has yet to be acknowledged.

Due to the relatively small number of trials performed by each subject, our ability to properly build models using training and testing was limited. Indeed, the size of our data did not allow for rigorous assessment to procure a fair assessment of decoding performance. Rather, what one should evaluate is the stability of the features selected, for in the event more data were to become available, the performance would improve but the features should remain.

We were able to establish a list of features that were found consistently between models. Overall, most of the regions selected as features have been found to be related to attention or performance monitoring in prior literature.

Specifically, angular gyrus has been implicated with attention and movement authorship [25], cingulate cortex with error processing [7], [26], hippocampus with memory and motor response [14] and the insular cortex with introspective error awareness and emotional saliency [26]. Further, cingulate gyrus, hippocampus, and insular cortex have been found to modulate activity based on learning from past errors [5]. Most features in the final models consisted of neural activity from the frequency bands alpha and low gamma. However, there was a shift from low gamma towards hyper gamma between planning to execution.

This work suggests that activity from nonmotor regions in our data can predict error, in terms of speed, prior to movement completion. Future work would go towards designing a more rigorous model building procedure and further investigating the relationship between behavior and neural activity as suggested by our models.

REFERENCES

[1] A. P. Georgopoulos, R. E. Kettner, and A. B. Schwartz, "Primate motor cortex and free arm movements to visual targets in three-dimensional space. II. Coding of the direction of movement by a neuronal population," *Journal of Neuroscience*, vol. 8, pp. 2928–2937, August 1988.

[2] M. A. Lebedev and M. A. Nicolelis, "Brain–machine interfaces: past, present and future," *TRENDS in Neuroscience*, vol. 29, pp. 536–546, September 2006.

[3] M. Corbetta and G. L. Shulman, "Control of goal-directed and stimulus-driven attention in the brain," *Nature Reviews Neuroscience*, vol. 3, pp. 201–215, March 2002.

[4] K. V. Shenoy, D. Meeker, S. Cao, S. A. Kureshi, B. Pesaran, C. A. Buneo, A. P. Batista, P. P. Mitra, J. W. Burdick, and R. A. Andersen, "Neural prosthetic control signals from plan activity," *Neuroreport*, vol. 14, pp. 591–596, March 2003.

[5] R. Hester, N. Barre, K. Murphy, T. J. Silk, and J. B. Mattingley, "Human medial frontal cortex activity predicts learning from errors," *Cerebral Cortex*, vol. 18, pp. 1933–1940, August 2008.

[6] J. Diedrichsen, Y. Hashambhoy, T. Rane, and R. Shadmehr, "Neural correlates of reach errors," *Journal of Neuroscience*, vol. 25, pp. 9919–9931, October 2005.

[7] A. Sapir, G. d'Avossa, M. McAvoy, G. L. Shulman, and M. Corbetta, "Brain signals for spatial attention predict performance in a motion discrimination task," *PNAS*, vol. 102, pp. 17810–17815, December 2005.

[8] N. K. Logothetis, "What we can do and what we cannot do with fMRI," *Nature*, vol. 453, pp. 869–878, June 2008.

[9] H. Scherberger, M. R. Jarvis, and R. A. Andersen, "Cortical local field potential encodes movement intentions in the posterior parietal cortex," *Neuron*, vol. 46, pp. 347–354, April 2005.

[10] N. F. Ince, R. Gupta, S. Arica, A. H. Tewfik, J. Ashe, and G. Pellizzer, "High accuracy decoding of movement target direction in non-human primates based on common spatial patterns of local field potentials," *PLoS One*, vol. 5, p. e14384, December 2010.

[11] L. M. Ward, "Synchronous neural oscillations and cognitive processes," *Trends in Cognitive Sciences*, vol. 7, pp. 553–559, Dec. 2003.

[12] J. González-Martínez, J. Bulacio, S. Thompson, J. T. Gale, S. Smithason, I. Najm, and W. Bingaman, "Technique, results, and complications related to robot-assisted stereoelectroencephalography," *Neurosurgery*, vol. 78, pp. 169–180, Sept. 2015.

[13] M. A. Johnson, S. Thompson, J. González-Martínez, H. J. Park, J. Bulacio, I. Najm, K. Kahn, M. Kerr, S. V. Sarma, and J. T. Gale, "Performing behavioral tasks in subjects with intracranial electrodes," *Journal of Visualized Experiments*, p. e51947, Oct. 2014.

[14] M. S. D. Kerr, P. Sacré, K. Kahn, H. J. Park, M. Johnson, J. Lee, S. Thompson, J. Bulacio, J. Jones, J. González-Martínez, C. Liégeois-Chauvel, S. V. Sarma, and J. T. Gale, "The role of associative cortices and hippocampus during movement perturbations," *Frontiers in Neural Circuits*, vol. 11, p. 26, 2017.

[15] M. S. Breault, P. Sacré, J. González-Martínez, J. T. Gale, and S. V. Sarma, "An exploratory data analysis method for identifying brain regions and frequencies of interest from large-scale neural recordings," *Journal of Computational Neuroscience*, pp. 1–15, December 2018.

[16] W. F. Asaad and E. N. Eskandar, "A flexible software tool for temporally-precise behavioral control in Matlab," *Journal of Neuroscience Methods*, vol. 174, pp. 245–258, Sept. 2008.

[17] E. Basar, C. Basar-Eroglu, S. Karakas, and M. Schurmann, "Brain oscillations in perception and memory," *International Journal of Psychophysiology*, vol. 35, pp. 95–124, Mar. 2000.

[18] R. T. Canolty and R. T. Knight, "The functional role of cross-frequency coupling," *Trends in Cognitive Sciences*, vol. 14, pp. 506–515, Nov. 2010.

[19] N. E. Crone, D. L. Miglioretti, B. Gordon, and R. P. Lesser, "Functional mapping of human sensorimotor cortex with electrocorticographic spectral analysis: II. Event-related synchronization in the gamma band," *Brain*, vol. 121, pp. 2301–2315, Dec. 1998.

[20] N. E. Crone, D. L. Miglioretti, B. Gordon, J. M. Sieracki, M. T. Wilson, S. Uematsu, and R. P. Lesser, "Functional mapping of human sensorimotor cortex with electrocorticographic spectral analysis: I. Alpha and beta event-related desynchronization," *Brain*, vol. 121, pp. 2271–2299, Dec. 1998.

[21] M. J. Kahana, D. Seelig, and J. R. Madsen, "Theta returns," *Current Opinion in Neurobiology*, vol. 11, pp. 739–744, Dec. 2001.

[22] S. L. Gonzalez, R. Grave de Peralta, G. Thut, J. del R Millán, P. Morier, and T. Landis, "Very high frequency oscillations (VHFO) as a predictor of movement intentions," *NeuroImage*, vol. 32, pp. 170–179, August 2006.

[23] I. Guyon and A. Elisseeff, "An introduction to variable and feature selection," *Journal of Machine Learning Research*, vol. 3, pp. 1157–1182, March 2003.

[24] S. Mori, S. Wakana, P. C. V. Zijl, and L. M. Nagae-Poetscher, *MRI atlas of human white matter*. Elsevier, May 2005.

[25] C. Farrer, S. H. Frey, J. D. V. Horn, E. Tunik, D. Turk, S. Inati, and S. T. Grafton, "The angular gyrus computes action awareness representations," *Cerebral Cortex*, vol. 18, pp. 254–261, February 2008.

[26] T. A. Klein, T. Endrass, N. Kathmann, J. Neumann, D. Y. von Cramon, and M. Ullsperger, "Neural correlates of error awareness," *NeuroImage*, vol. 34, pp. 1774–1781, 2006.